Complex burrows of the mud shrimp *Callianassa truncata* and their geochemical impact in the sea bed

W. Ziebis, S. Forster, M. Huettel & B. B. Jørgensen

Max Planck Institute for Marine Microbiology, Celsiusstrasse 1, D-28359 Bremen, Germany

THE biogeochemical processes and associated microbial communities in the sea floor are stratified[1] and dependent on vertical transport mechanisms. The penetration of oxygen is generally only a few millimetres in coastal sediments[2], regulated by the dynamic balance between diffusion from the overlying water and rapid consumption within the sea bed. Macrofauna organisms living within the sea bed affect the physical structure of the sea floor, its chemical zonations and the exchange processes across the sediment–water interface[3,4]. Thalassinidean mud-shrimps are often abundant in tropical and temperate coastal regions[5–7] and build burrows with a species-specific architecture. The deepest reported burrows reach down to 2.5 m sediment depth[8]. It is difficult to study the activities of these secretive animals and their effect on sediment biogeochemistry without disturbing the sediment system[9]. Here we report the use of a diver observatory within the seabed, along with *in situ* measurements, to assess the geochemical impact of the mud-shrimp *Callianassa truncata* Giard and Bonnier (Decapoda, Thalassinidea), a species that commonly inhabits sandy sediments in the Mediterranean sea.

An interesting underwater landscape created by the mud shrimp, *Callianassa truncata*, was found in a shallow bay off the coast of the Italian island, Giglio, in the Mediterranean Sea (Fig. 1). Conspicuous mounds and funnels covered the sea bed at an average density of 120 mounds per square metre (± 43, $n = 240$). One mound and two funnels constitute the surface structure of one burrow system, built and maintained by a single shrimp (Fig. 1).

Polyester resin casts revealed that the intricate burrows have a uniform architecture of horizontal galleries interconnected by vertical shafts (Fig. 2*a*). The first horizontal gallery is connected to the overlying water[10] and consists of three connected chambers aligned in roughly 10 cm sediment depth (Fig. 2*b*). From two funnels, slanted inhalant shafts lead to the first spherical chamber. The third chamber is elongated and narrows into a thin exhalant tube, which bends at a right angle straight up to the sediment surface and ends at the top of a conical mound. From the central chamber, the burrow continues vertically downward with 7–10 galleries, each consisting of 2–5 spherical chambers at regular depth intervals and it ends blindly in a single chamber.

At the observed abundances (120 per m^2) the extensive burrows, with a mean volume of 60 cm^3 (± 5 cm^3, $n = 14$), increase the total area of the sediment–water interface by roughly 400%. In the course of burrowing, fine-grained sediment is selectively excavated and ejected to the sediment surface through the thin shaft in the mound. Before ejection, the sand grains are gleaned for organic matter. Coarse grains, possibly too heavy to be ejected, are transported downward and are used for the construction of the chamber walls at deeper burrow levels (Fig. 2*a*, insert). The selective ejection of fine-grained sand into the overflowing sea water increases the bulk sediment permeability of the inhabited area. As the depth intervals of galleries are very regular for all burrows, the accumulation of coarse sand grains in chamber walls resulted in distinct layers of highly permeable coarse sand. Such high permeability facilitates pore-water flow and is thus an important factor for solute exchange in sediments.

The biogenic surface topography alters the small-scale flow regime of the bottom current[11]. The boundary flow accelerates

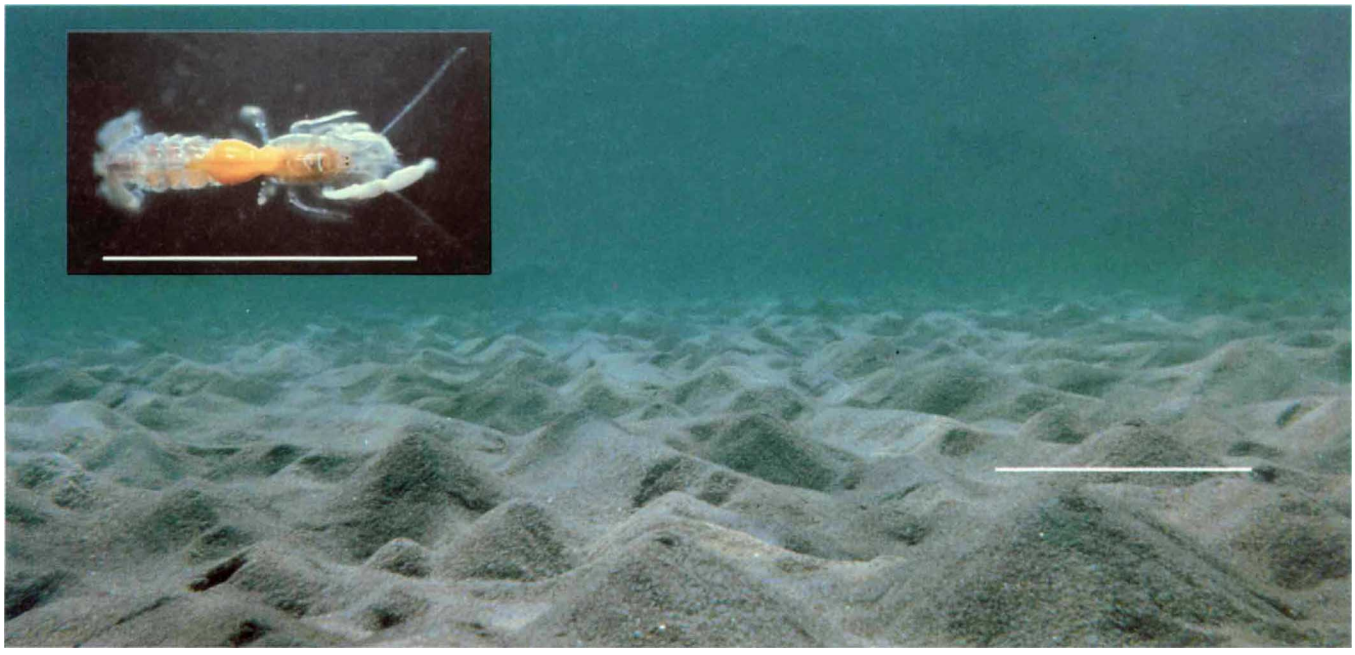

FIG. 1 Sediment surface topography at 5-m water depth created by the burrowing shrimp, *Callianassa truncata* (insert), in the bay of Campese, Isola del Giglio, Italy (42° 20′ N, 10° 52′ E). Conical mounds with an average height of 4 cm (maximum 9 cm) and funnel-shaped depressions (average depth 4 cm, maximum 6 cm) cover the sea bed between 2 and 15 m water depth in the entire bay. The upper 10 cm of bulk sediment consists of organically poor sand (0.2% dry weight) which is well sorted with a median grain size of 350 μm. The volcano-shaped mounds consist of finer sand (median grain size, 200 μm) than the ambient sediment and are created from discarded sediment which is ejected by the animals at the excurrent openings of their burrows. On average, 2–3 kg of sand per m^2 and per day were ejected up to 6 cm up into the bottom-water current, ranging in velocity from 2 to 16 cm s^{-1}, as recorded 5 cm above the sea bed in the months from May to August. Scale bars, 10 cm (sediment) and 2 cm (insert). Photograph by Thomas Pillen.

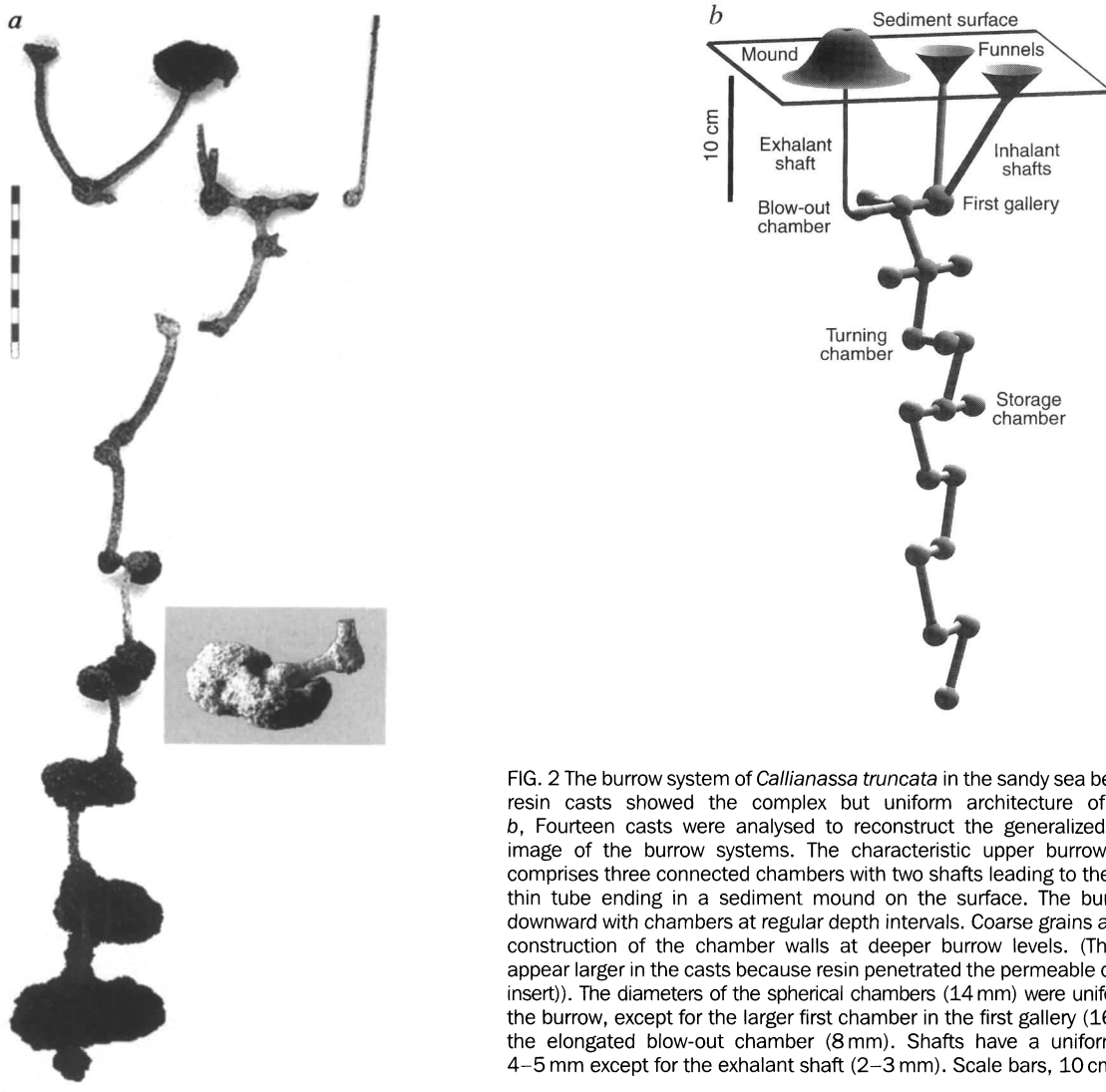

FIG. 2 The burrow system of *Callianassa truncata* in the sandy sea bed. *a*, Polyester resin casts showed the complex but uniform architecture of the burrows. *b*, Fourteen casts were analysed to reconstruct the generalized 3D computer image of the burrow systems. The characteristic upper burrow compartment comprises three connected chambers with two shafts leading to the funnels and a thin tube ending in a sediment mound on the surface. The burrow continues downward with chambers at regular depth intervals. Coarse grains are used for the construction of the chamber walls at deeper burrow levels. (These chambers appear larger in the casts because resin penetrated the permeable coarse walls (*a*, insert)). The diameters of the spherical chambers (14 mm) were uniform throughout the burrow, except for the larger first chamber in the first gallery (16–17 mm) and the elongated blow-out chamber (8 mm). Shafts have a uniform diameter of 4–5 mm except for the exhalant shaft (2–3 mm). Scale bars, 10 cm.

when passing over a mound but is retarded in the upstream and downstream regions. The resulting lateral velocity gradients cause pressure differences that drive advective pore-water flows[12–14]. In the high-pressure areas, oxygen-rich supernatant water is forced into the permeable sediment and flows in a curved path towards the lee side of the mound where anoxic pore water emerges because of the lower pressure. Pore-water solutes, such as nutrients or metal ions are thereby released into the water column. The local advective solute transport by far exceeds the molecular diffusion across the sediment–water interface.

The flow pattern and the resulting oxygen distribution was studied around a *Callianassa* mound that had been established in sediment cores from the natural habitat and placed within a laboratory flow channel (Fig. 3). Oxygen was transported roughly 40 mm by the advective pore-water flow, whereas oxygen penetration at a smooth surface did not exceed 4 mm. In the high-pressure areas, upstream and downstream of the mound, high oxygen concentrations (>100 μM) persisted to a sediment depth of 20 mm. The sediment volume adjacent to a mound of height 1 cm that was supplied with oxygen under a current of 10 cm s^{-1} was calculated to be 90 cm^3 and thereby increased locally 4.5-fold compared to the oxic zone underneath a flat surface. The availability of oxygen for aerobic degradation processes was thus enhanced in the flume sediment with 22 mounds per m^2 by a factor of 1.5. This explained a 1.7-fold increase in total oxygen uptake of this sediment measured in the water column of a gas-tight sealed flume compared to a smooth sediment in a parallel set-up. The lateral velocity gradients of the bottom-water flow also caused a passive ventilation[14,15] of the upper part of the burrow system. Because of the low pressure, burrow water was sucked out through the exhalant opening on top of the mound. A compensating inflow of oxygen-rich water occurred through the funnel openings. The hydrodynamically induced water flow had a velocity of 0.3–0.4 cm s^{-1} in the inhalant shafts and about twice that in the exhalant tube. Organic material, mainly sea-grass debris, was physically trapped in the funnels. The shrimps either feed directly on the organic material and the associated bacteria or store it in blind chambers of the burrow system for further microbial decomposition. This active downward transport provided a fast burial of organic material in the sea bed.

In addition to the hydrodynamically induced flushing, the shrimps produce a water current through their burrow system by a regular beating of their pleopods. Until now it was not known how deep oxygen was transported into the burrows and how far it penetrated into the surrounding sediment and thus how it affected the geochemistry. *In situ* studies were therefore done. A hexagonal acrylic observatory, large enough to accommodate one or two SCUBA divers, was buried 1.2-m deep in the sand with its lid level with the sediment surface. Two months after deployment, the surrounding sediment had been reinhabited by *C. truncata* at natural densities. Silicone-filled holes in the acrylic walls allowed direct sampling and measurements in intact burrows. Oxygen microelectrodes[16] were inserted horizontally into the burrows and the surrounding sediment using micromanipulators. Contin-

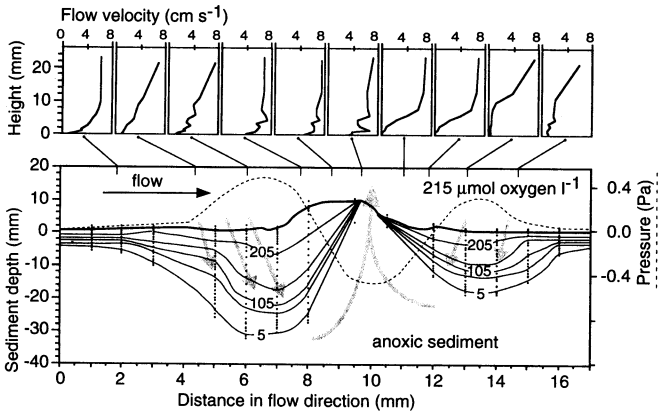

FIG. 3 Water flow and oxygen distribution around a 1-cm high *Callianassa* mound. Upper graph: flow velocity profiles; lower graph: oxygen (isopleths) and hydrodynamic pressure distribution. Measurements were taken in a laboratory flow channel (200 × 30 × 12 cm) containing a natural sediment core (60 × 30 × 20 cm; median grain size, 350 µm, permeability *k* (defined as a material constant related to the pore size of a sediment by the tortuosity factor[20]) = 5.1×10^{-11} m^2; porosity, 0.4) inhabited by *C. truncata*. The surface of the sediment core was level with the channel floor. Flow velocities were measured at 1 mm vertical resolution using a thermistor probe[18]. Fourteen oxygen profiles (vertical dotted lines) were recorded using Clark-type microelectrodes[15] driven into the sediment at 250 µm depth increments. The isopleths connect points of equal oxygen concentration at 50 µM intervals. Fifteen pressure ports were located at the sediment–water interface and connected to a differential pressure gauge by which the pressure distribution over the mound was measured. Grey arrows indicate the flow paths of water and pore fluid. Oxygen penetrated down to 38 mm, whereas oxygen penetration did not exceed 4 mm in the area not affected by the mound.

uous oxygen measurements at 26 cm and 48 cm sediment depth revealed that *C. truncata* maintained burrow-water oxygen concentrations at 10–40% and 3–12% of air saturation, respectively, at the two depths (Fig. 4*a*). Horizontal oxygen microelectrode profiles measured in steps of 250 µm perpendicular to the burrow showed that oxygen penetrated 6–7 mm through the highly permeable chamber walls into the ambient sediment, whereas oxygen penetration out from the vertical shafts was only 3 mm at both depths (Fig. 4*b*, *c*). An oxic sediment environment of 12–25-mm diameter thus surrounds each burrow. Given the population density of 120 individuals per m^2, each 10 cm × 10 cm area of the seabed thus contained one complex structure, some centimetres wide, of oxic sediment penetrating down at least half a metre.

By the active exchange of burrow water, products of organic degradation, such as ammonium, are efficiently transported into the overlying water. The flushing with oxygenated seawater also enhances the bacterial ammonium oxidation and probably other bacterial activities in the sediment[17]. Ammonium concentrations measured inside the burrows were thus low (2–14 µmol l^{-1}) down to a depth of 60 cm. In the pore water of the surrounding sediment, ammonium was depleted to <15 µmol l^{-1} at a distance of up to 3–4 cm as compared with 100 µmol l^{-1} in surrounding sediment not inhabited by *C. truncata*. The depletion affects a sediment column of roughly 10 cm diameter around each burrow. At the observed abundance, the ammonium concentration was thus kept low in the entire sediment down to at least 50-cm depth (Fig. 4). The oxygenation of the sediment caused by the bioirrigation by *C. truncata* was also apparent from the marked differences

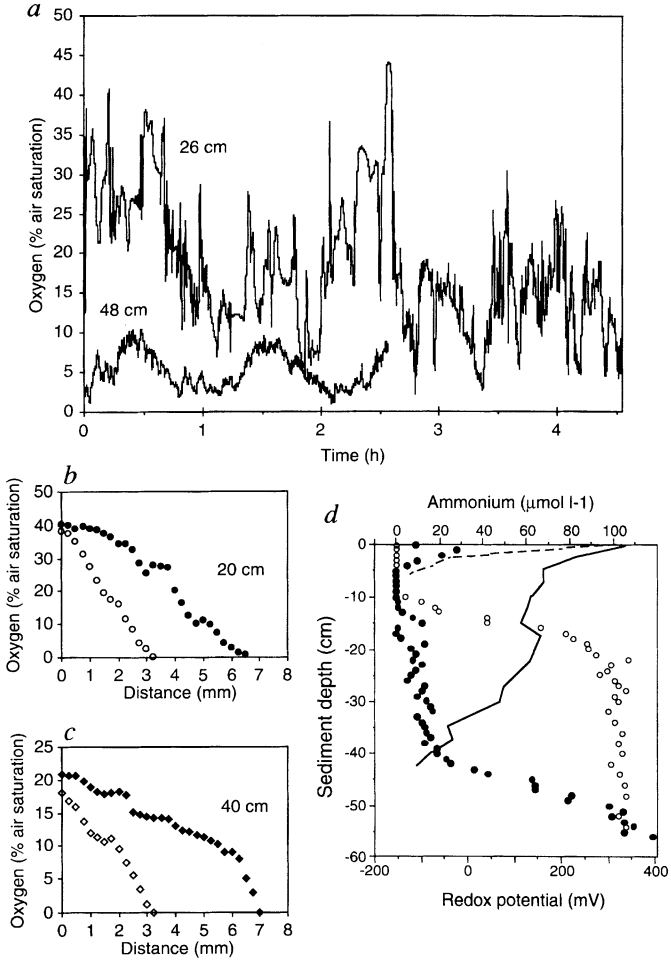

FIG. 4 *a*, Continuous oxygen measurements within a burrow system at 26 cm and 48 cm sediment depth. *b*, *c*, Oxygen micro-profiles measured at roughly 20 and 40 cm sediment depths from inside the burrow and out through chamber walls (●, ♦) and tube walls (○, □) into the surrounding sediment. These measurements were made *in-situ* from a hexagonal observatory (1.2 m high, 2 m diameter) deployed in the sea bed at 5-m water depth. Six acrylic walls allowed direct observations and measurements through silicone-filled holes. Continuous oxygen data were recorded by a 12-bit data logger. The instruments were self-contained in water-tight housings. One electrode was inserted into the burrow lumen and a second electrode was introduced into the ambient sediment at the same depth. This control showed that oxygen did not penetrate through the silicone ports and that measurements inside the burrows thus represented true *in situ* concentrations. *d*, Redox and ammonium profiles in sediment inhabited (— and ●) by *C. truncata* compared to profiles in a non-inhabited (- - - and ○) sediment. The latter was established in cages, with 1-mm mesh size to exclude the macrofauna, which were attached to the wall outside the observatory. Ammonium samples were taken with evacuated serum vials closed with silicone stoppers. Using two connected syringes with a filter (pore size, 45 µm) in between, small samples (1 ml) were sucked into the vial by inserting one end into the burrow or sediment through the silicone ports in the observatory walls, while the other end penetrated through the silicone stopper into the vial. Samples were analysed within 24 h by the flow-injection method modified for small samples[19]. Redox potentials in the bulk sediment were measured using platinum electrodes inserted through silicone stoppers in the acrylic glass walls at vertical steps of 1 cm down to 56-cm sediment depth.

in redox potential existing between inhabited and non-inhabited sediment (Fig. 4*d*).

The *in-situ* studies from our sediment observatory revealed that the mud shrimp, *C. truncata*, although only 2-cm long, constructs unique burrows of extreme architectural and functional complexity that influence the whole sedimentology and geochemistry of the sea bed. The design of the upper burrow system, including mounds, funnels and first gallery, induces a hydrodynamic water exchange in the upper sediment layer. The biopumping of dissolved oxygen down to 60–80 cm sediment depth and the transport of detrital particles to similar depths can strongly accelerate the degradation of organic matter in the sandy sediments. □

Received 22 February; accepted 8 July 1996.

1. Berner, R. A. *Early Diagenesis: A Theoretical Approach* (Princeton Univ. Press, Princeton, 1980).
2. Revsbech, N. P., Jørgensen, B. B. & Blackburn, P. H. *Science* **207,** 1355–1356 (1980).
3. Aller, R. C. in *Animal–Sediment Relations* (eds McCall, P. L. & Tevesz, M. J. S.) 53–104 (Plenum, London, 1982).
4. Boudreau, B. P. *Geochim. Cosmochim. Acta* **58,** 1243–1249 (1994).
5. Aller, R. C. & Dodge, R. E. *J. Mar. Res.* **32,** 209–232 (1974).
6. Griffis, R. B. & Suchanek, T. H. *Mar. Ecol. Prog. Ser.* **79,** 171–183 (1991).
7. Dworschak, P. C. *Mar. Ecol.* **4,** 19–43 (1983).
8. Pemberton, S. G., Risk, M. J. & Buckley, D. E. *Science* **192,** 790–791 (1976).
9. Forster, S. & Graf, G. *Mar. Biol.* **123,** 335–346 (1995).
10. Ray, A. J. & Aller, R. C. *Mar. Geol.* **62,** 371–379 (1985).
11. Schlichting, H. *Boundary Layer Theory* 7th edn (McGraw-Hill, New York, 1987).
12. Huettel, M. & Gust, G. *Mar. Ecol. Prog. Ser.* **89,** 253–267 (1992).
13. Yager, P. L., Nowell, R. A. M. & Jumars, P. A. J. *J. Mar. Res.* **51,** 209–236 (1993).
14. Vogel, S. *Life In Moving Fluids* (Princeton Univ. Press, New Jersey, 1983).
15. Allanson, B. R., Skinner, D. & Imberger, J. *Est. Coast. Shelf Sci.* **35,** 253–266 (1992).
16. Revsbech, N. P. *Limnol. Oceangr.* **34,** 474–478 (1989).
17. Kristensen, E. J. *Coast. Res.* **1,** 109–116 (1985).
18. LaBarbera, M. & Vogel, S. *Limnol. Oceanogr.* **21,** 750–756 (1976).
19. Hall, P. O. J. & Aller, R. C. *Limnol. Oceanogr.* **37,** 1113–1119 (1992).
20. Hsü, K. J. *Physical Principles of Sedimentology* (Springer, Berlin, Heidelberg, 1989).

ACKNOWLEDGEMENTS. We thank T. Pillen and B. Unger for the construction and deployment of the diver observatory and for their help during underwater field work, other members of the Giglio Diving and Research Team: D. Claus, K. Eichstaedt, J. Hass and C. Lott; and A. Eggers, G. Eickert, O. Goerg, A. Glud, G. Herz, G. Kothe and V. Meyer for technical support and the construction of microelectrodes. The study was supported by the Max Planck Society.

CORRESPONDENCE and requests for materials should be addressed to W.Z. (e-mail: wiebke@postgate.mmi-mm.uni-bremen.de).

Genetically lean mice result from targeted disruption of the RIIβ subunit of protein kinase A

David E. Cummings, Eugene P. Brandon, Josep V. Planas, Kouros Motamed, Rejean L. Idzerda & G. Stanley McKnight

Department of Pharmacology, University of Washington School of Medicine, Seattle, Washington 98195–7750, USA

Cyclic AMP is an important second messenger in the coordinated regulation of cellular metabolism. Its effects are mediated by cAMP-dependent protein kinase (PKA), which is assembled from two regulatory (R) and two catalytic (C) subunits. In mice there are four R genes (encoding RIα, RIβ, RIIα, and RIIβ) and two C genes (encoding Cα and Cβ), expressed in tissue-specific patterns[1]. The RIIβ isoform is abundant in brown and white adipose tissue and brain, with limited expression elsewhere. To elucidate its functions, we generated RIIβ knockout mice. Here we report that mutants appear healthy but have markedly diminished white adipose tissue despite normal food intake. They are protected against developing diet-induced obesity and fatty livers. Mutant brown adipose tissue exhibits a compensatory increase in RIα, which almost entirely replaces lost RIIβ, generating an isoform switch. The holoenzyme from mutant adipose tissue binds cAMP more avidly and is more easily activated than wild-type enzyme. This causes induction of uncoupling protein and elevations of metabolic rate and body temperature, contributing to the lean phenotype. Our results demonstrate a role for the RIIβ holoenzyme in regulating energy balance and adiposity.

RIIβ null mutant mice were generated by targeted gene disruption; details of the knockout construction will be published elsewhere. Western blotting confirmed the absence of RIIβ protein in homozygous mutants. RIIβ mutants are fertile and long lived, exhibiting no overt abnormal phenotype. However, they have remarkably decreased white adipose tissue (WAT) mass. The weights of fat pads from three anatomical locations in mutants were about half those of the wild types (Table 1). Magnetic resonance imaging (Fig. 1*a*) confirmed that the reduction in fat occurs throughout the whole body. Whole-mouse magnetic resonance spectroscopy[2] and volume-of-distribution experiments with ^3H_2O showed that mutants have approximately 6% body fat, compared with 15% in the wild type.

The knockout mice are not cachectic. Overall weight is reduced by suggesting ~10%, that loss of fat is probably the only alteration in body composition (Table 1). Leanness does not seem to result from decreased food intake or absorption. Mutants tend to be slightly hyperphagic (Table 1), and show normal postprandial triglyceride blood levels. Plasma cholesterol, free fatty acids, insulin, glucose and thyroid hormones are also unperturbed (data not shown). The reduction of WAT seems to arise principally from decreased triglyceride stores, rather than diminished

TABLE 1 Knockout mice have reduced adipose tissue mass

	Reproductive fat-pad weight (% body weight)	Inguinal fat-pad weight (% body weight)	Retroperitoneal fat-pad weight (% body weight)	Reproductive fat-pad cellularity ($\times 10^{-6}$ cells per pad)	Inguinal fat-pad cellularity ($\times 10^{-6}$ cells per pad)	Retroperitoneal fat-pad cellularity ($\times 10^{-6}$ cells per pad)	Body weight (g)	Food intake (kcal per mouse per d)
Male								
Wild type	1.29 ± 0.10	0.96 ± 0.10	0.29 ± 0.04	17.4 ± 0.9	18.6 ± 1.9	3.7 ± 0.5	25.2 ± 0.9	11.4 ± 2.7
Mutant	0.62 ± 0.04	0.63 ± 0.04	0.11 ± 0.01	15.4 ± 1.5	21.4 ± 2.6	3.4 ± 0.5	23.4 ± 1.1	12.4 ± 1.5
% of wild type	48%	65%	37%	89%	115%	92%	93%	109%
	$P \leq 0.0001$	$P \leq 0.002$	$P \leq 0.0001$	$P = 0.14$	$P = 0.21$	$P = 0.31$	$P = 0.10$	$P = 0.39$
Female								
Wild type	2.25 ± 0.34	1.09 ± 0.03	0.23 ± 0.02	19.0 ± 2.0	21.6 ± 2.3	ND	22.4 ± 1.7	9.1 ± 0.4
Mutant	0.97 ± 0.13	0.72 ± 0.04	0.11 ± 0.02	17.4 ± 1.7	21.1 ± 2.8	ND	19.5 ± 0.8	10.9 ± 0.3
% of wild type	43%	66%	48%	92%	98%		87%	120%
	$P \leq 0.0006$	$P \leq 0.0001$	$P \leq 0.001$	$P = 0.21$	$P = 0.44$		$P = 0.06$	$P = 0.01$

RIIβ null mutants have reduced adipose tissue mass despite adequate food intake. Discrete white fat pads from three anatomical sites were dissected and weighed. 'Reproductive' refers to the epididymal and parametrial pads of males and females, respectively. White adipose tissue cellularity was ascertained by DNA quantitation. Consumption of standard mouse chow (Harlan Teklad) was measured over four months starting at six weeks of age. Results are means ± s.e.m.